Matrix isolation and theoretical study on the photolysis of trichloroacetyl chloride

Takumi Tamezane, Nobuaki Tanaka*, Hiromasa Nishikiori, Tsuneo Fujii

Department of Environmental Science and Technology, Faculty of Engineering, Shinshu University, 4-17-1 Wakasato, Nagano, Nagano 380-8553, Japan

Received 25 October 2005; in final form 31 March 2006

Abstract

UV photolysis of CCl_3COCl has been investigated by infrared spectroscopy in cryogenic Ar and O_2 matrices. In the Ar matrix, CCl_4 and CO were found to be dominant products over $Cl_2C=C=O$. The CCl_3 and COCl species, observed as intermediates, indicated C-C bond cleavage. The C-C bond cleavage was also evidenced by the formation of ClC(O)OO in the O_2 matrix. The marked difference in the photochemistry of matrix-isolated CCl_3COCl from that of CH_3COCl, where $CH_2=C=O$ is the predominant product, can be attributed to the triplet surface reaction of CCl_3COCl, as supported by the present DFT calculations.

* Corresponding author. Tel: +81-26-269-5527, Fax: +81-26-269-5550
E-mail: ntanaka@shinshu-u.ac.jp

1. Introduction

Since chlorinated acetyl chlorides play important roles in the photochemical reactions of chlorinated ethenes [1-5], their photolysis reactions have been studied actively, especially in environmental concern. In the photochemical reaction of acetyl chloride, CH_3COCl, in matrices [6,7], acetyl chloride was photoexcited by irradiation of 266 nm laser to the S_1 state, which suffered internal conversion and decomposed to the HCl· ketene complex in the S_0 state [7]; four-center elimination mechanism was proposed for this process. In the gas phase, rapid C(O)-Cl dissociation (< 200 fs) occurs upon 253 nm irradiation [8]. In the CF_3COCl photolysis, CF_3Cl and CO were produced via the radical mechanism [9]. As for the thermal reaction, vacuum pyrolysis of CCl_3COCl at 970-1370 K showed primary processes to CCl_3 + COCl and Cl_2 + $Cl_2C=C=O$ [10]. However, there is as yet only limited understanding on the photochemical processes of acetyl chloride derivatives, especially on the role of halogen substituents in their reactions in electronic excited states.

In this Letter we report on the photochemical reaction of CCl_3COCl in cryogenic matrices as a prototype of chlorinated acetyl chloride. In order to discrimate the concerted mechanism from the radical mechanism, we have used the O_2 matrix as a reaction medium as well as the Ar matrix. We have also made density functional theory (DFT) calculations for spectral analysis and for discussion on the reaction mechanism.

2. Experimental

Ultraviolet (UV) irradiation was performed using a low-pressure mercury arc lamp (HAMAMATSU L937-02). Infrared (IR) spectra were measured in the range 4000-700 cm^{-1} with 1.0 cm^{-1} resolution by a SHIMADZU 8300A Fourier transform IR spectrometer with a liquid-nitrogen-cooled MCT detector. Each spectrum was obtained by scanning over 128 times. A closed-cycle helium cryostat (Iwatani M310/CW303) was used to control the temperature of the matrix.

Argon gas (Air Liquide, >99.9998%) and O_2 (Okaya Sanso) were used without further purification. Trichloroacetyl chloride (Wako Pure Chemicals) was used after freeze-pump-thaw cycling at 77 K. Carbon tetrachloride (Wako Pure Chemicals) was used as an authentic sample for product identification. Samples were deposited on a CsI window at 6 K.

For product identification and energetic consideration, molecular orbital calculation was utilized. Geometry optimizations were performed using Becke's three-parameter

hybrid density functional [11] in combination with the Lee-Yang-Parr correlation functional, B3LYP [12] with the aug-cc-pVTZ basis set. Calculations of harmonic vibrational frequencies were performed to confirm the predicted structures as local minima or a transition state (one imaginary frequency) and to elucidate zero-point vibrational energy corrections (ZPE). The obtained transition states were confirmed as those connecting with the desired species by calculation of subsequent intrinsic reaction coordinates. The CIS method was employed for the optimization of the S_1 state. Vertical excitation energy was calculated at the CIS and TD-B3LYP levels. All calculations were performed using Gaussian 03W [13].

3. Results and discussion

3.1. CCl_3COC in the Ar matrix

A mixture of CCl_3COCl/Ar was deposited on a CsI window with a ratio of CCl_3COCl/Ar = 1/1000. In the IR spectrum obtained after deposition, strong bands were observed at 1807.7, 1026.5, 856.8-851.5, 807.6-801.4 and 750.3-740.6 cm^{-1} assignable to the vibrational modes of C=O stretching, C-C stretching, CCl_3 a" anti stretching, CCl_3 a' anti stretching and C-Cl stretching, respectively according to Fausto [14].

The IR difference spectrum obtained upon UV irradiation of a CCl_3COCl/Ar matrix for 60 min is shown in Fig. 1. The positive and negative bands indicate the growth and depletion, respectively, during the irradiation period. The observed wavenumbers of the product bands are listed in Table 1. A strong band observed at 2137 cm^{-1} assignable to CO stretching continued to grow during the prolonged irradiation period. A band at 2155 cm^{-1} showed growth and decay behavior accompanied with the 1293 and 934 cm^{-1} bands, whose wavenumbers are consistent with those of $Cl_2C=C=O$ within 3 cm^{-1} [10]. Bands appearing at 2151, 1286 and 936 cm^{-1} with a slower growth rate, which are distinguishable from the above three bands, are assigned to those of $Cl_2C=C=O$ placed in a different environment. In the carbonyl C=O stretching region, a band at 1814 cm^{-1} overlapping with the CCl_3COCl depletion band at 1807.7 cm^{-1} concurrently increased with the 837 cm^{-1} band, which is assignable to $COCl_2$ [15]. A band at 1878 cm^{-1} was assigned to COCl ν_1 [16]. The weak 1969 cm^{-1} band showing an induction period might be the ν_1 of CCO [17]. In the 1000-700 cm^{-1} region, two clear bands at 788 and 767 cm^{-1} grew maintaining the same relative intensities during the irradiation period; they were attributed to a single molecule, which was identified with CCl_4 by comparison with the authentic spectrum measured in argon matrix. A strong band at 899 cm^{-1}

accompanied with a weak band at 864 cm^{-1} was assigned to CCl_3 ν_3 [18]. Very weak bands at 2139, 1036 and 929 cm^{-1} showed the same time profile, indicative of a single species. The wavenumber of 2139 cm^{-1} is very close to that of CO. Bands at 1036 and 929 cm^{-1} are comparable with those at 1019.7 and 929.1 cm^{-1} of $Cl_2CCl\cdots Cl$ [19]. The 1036 cm^{-1} band is also comparable with the 1036.6 cm^{-1} band of CCl_3^+ [20]. Based on this comparison, this species is tentatively identified with $Cl_2CCl\cdots Cl\cdots CO$. After prolonged irradiation, a trace amount of the CCl_2=CCl_2 bands appeared at 916 cm^{-1}, presumably due to the recombination of reactive CCl_2.

Figure 2 compares the time evolution of the photolysis product yields of CCl_3 and CCl_4 measured in the annealed matrix before irradiation and non-annealed matrix upon reduced irradiation. The induction period is discernible in the CCl_4 growth displayed in the non-annealed matrix, (b), whereas no such period exists in the annealed matrix, where CCl_3 formation is depressed. Abstraction of the Cl atom from the COCl cage partner by the CCl_3 to form CCl_4 and CO must be enhanced by the effect of annealing.

3.2. CCl_3COCl in the O_2 matrix

The photolysis in the O_2 matrix seems to include much more information about which bond cleaves predominantly. The amounts of CCl_3COCl photolyzed upon 360 min irradiation were 66% in Ar and 30% in O_2. A relatively smaller rate observed in the O_2 matrix may be attributed to the filter and triplet quencher effects of O_2. In the IR difference spectrum obtained after 60 min irradiation, Fig. 3, ozone formation is prominent at 1038 cm^{-1} due to the photolysis in O_2 at 253.7 nm [21]. A comparison of the ratio of CCl_4 or CO absorbance to CCl_3COCl absorbance with that in Fig. 1 indicates that the formation of CO and CCl_4 was depressed and that of CCl_3 and Cl_2C=C=O was negligible in the O_2 matrix. Instead, major products are found to be CO_2 and $COCl_2$. They are probably produced via reactions of COCl and CCl_3 with O_2, respectively. Several products appeared in addition to these species. A broad and weak band at 1436 cm^{-1} is assigned to ClOO ν_1 [22]. The formation of ClOO suggests the possibility of minor path involving the C(O)-Cl or CCl_2-Cl bond cleavage. The bands of 1888, 1824, 954 and 926 cm^{-1}, which were outstanding in an early stage of the photolysis agreed well with those of 1886, 1824, 952 and 925 cm^{-1}, respectively, for ClC(O)OO measured in the Ar matrix [23]. The 2037 cm^{-1} band is attributed to CO_3, though the band is slightly shifted from 2045 cm^{-1} observed in the CO_2 matrix [24]. Tso and Lee assigned the 2036 cm^{-1} band to the ν_1 of complexed CO_3 arising from the H_2CO photolysis in the O_2 matrix [25]. In the present case, CO_3 is likely to exist as

CO_3···Cl, whose structure is calculated to be planar at the UB3LYP/aug-cc-pVTZ level.

3.3. Reaction mechanism

Judging from the calculated IR intensities of 82, 513 and 618 km mol^{-1} for CO (2211 cm^{-1}), CCl_4 (734 cm^{-1}) and $Cl_2C=C=O$ (2217 cm^{-1}), respectively, it has been confirmed that the formation of CO and CCl_4 is the dominant process over the $Cl_2C=C=O$ formation in the Ar matrix.

In the CCl_3COCl/Ar system, we have found that the C-C bond-cleaved products, CCl_3, COCl, CCl_4 and CO, are dominant, contrary to the photolysis of acetyl chloride in the Ar matrix [7], where ketene formation was found to be the major process. Further evidence has been obtained from the CCl_3COCl/O_2 photolysis. The absence of $Cl_2C=C=O$ observed in the O_2 matrix indicates the $Cl_2C=C=O$ formation via the radical mechanism instead of the concerted mechanism. It seems plausible to explain the dominant radical mechanism via the triplet state by the enhanced intersystem crossing from S_1 caused by substitution of the chlorine atoms with methyl hydrogen atoms of acetyl chloride. On the S_1 surface the C-C bond cleavage does not yield the ground state product pair and hence is energetically inaccessible. Therefore, we focus on the triplet surface reaction after intersystem crossing and the ground state reaction after internal conversion.

Figure 4 shows the energy diagram for CCl_3COCl photolysis initiated by 253.7 nm irradiation. The reaction enthalpies of three elementary reactions from the T_1 equilibrium state are calculated to be –3.9, –20.3 and –25.9 kcal mol^{-1} for the C(O)-Cl, C-C and CCl_2-Cl bond cleavages, respectively, where the reaction barriers are 4.1, 6.2 and 2.8 kcal mol^{-1}, respectively. As opposed to the observed results, the C-C dissociation on the T_1 surface possesses the highest barrier. Contrary to the observed results, CCl_2-Cl bond cleavage seems to be the most favorable thermodynamically. Radical species CCl_3 and COCl can be produced not only from the C-C bond cleavage but also from the dissociation of CCl_3CO into CCl_3 and CO, followed by the recombination of CO with Cl. Theoretical calculations predict the Cl_2CCl···Cl···CO complex formation by the C-C bond elongation on the S_0 potential surface, which supports the identification. A negligible amount of CCl_3COCl would undergo the dissociation on S_0 after the internal conversion or intersystem crossing. According to this analysis, the charge distribution is described as $CCl_3^{\delta+}$···$Cl^{\delta-}$ in the complex. In the O_2 matrix, photofragments will undergo further reaction with O_2 and decomposition reaction.

To clarify the contradiction between the observation and energetic consideration, we consider the structural change upon excitation and potential surfaces. The electron configuration of S_1 is calculated to be $n_O\pi^*$ for the nascent C_s structure after photoexcitation while those of T_1 and T_2 to be $n_O\pi^*$ and $n_{Cl}\pi^*$, respectively, where the T_2 energy level is only 0.7 kcal mol^{-1} higher than the S_1 level. At the equilibrium structure for the S_1 state, the T_2 energy level is calculated to be situated 17.4 kcal mol^{-1} below the S_1 level. The C-O bond length for the S_1 equilibrium structure calculated at the CIS/6-311+G(2d) level is 0.092 Å longer than that of the ground state calculated at the HF/6-311+G(2d), corresponding to the $n_O\pi^*$ excitation character of S_1 as shown in Fig. 5. In addition, the change in the calculated C-C bond length, from the S_0 to the S_1 state, is remarkable 1.549 and 1.513 Å, whereas that in the C(O)-Cl bond length is insignificant. Just after the excitation on the S_1 surface, the C-C and C-O stretching vibrations coupled with the ClCCO torsion and CCOCl inversion vibrations are promoted to form the pyramidal S_1 equilibrium structure. It seems reasonable to assume that these vibrational modes are candidates of the dissociation reaction coordinate. It is supported by the normal mode analysis of the C-O stretching mode of S_1, where the potential energy distribution of the C-O and C-C stretching modes are calculated to be 29.9 and 11.3%, respectively. Along with the reaction coordinate, there appear points where the T_2 surface crosses the S_1 surface. The S_1-T_2 intersystem crossing caused by a spin-orbit interaction may proceed favorably, being followed by T_2-T_1 internal conversion toward dissociation.

In the present study, substitution of three chlorine atoms on acetyl chloride is found to alter the reaction mechanism. It provides the question on how many chlorine atoms are required for the triplet state reaction.

References

[1] S.Y. Nishida, S. Cervera-March, K.J. Nagano, M.A. Anderson, K. Hori, J. Phys. Chem. 99 (1995) 15814.

[2] P.B. Amama, K. Itoh, M. Murabayashi, J. Mol. Catal. A: Chem. 176 (2001) 165.

[3] K. Oki, S. Tsuchida, H. Nishikiori, N. Tanaka, T. Fujii, Int. J. Photoenergy 5 (2003) 11.

[4] A.S. Hasson, I.W.M. Smith, J. Phys. Chem. A 103 (1999) 2031.

[5] K.S. Wiltshire, M.J. Almond, P.C.H. Mitchell, Phys. Chem. Chem. Phys. 6 (2004) 58.

[6] N. Kogure, T. Ono, E. Suzuki, F. Watari, J. Mol. Struct. 296 (1993) 1.

[7] B. Rowland, W. P. Hess, J. Phys. Chem. A 101 (1997) 8049.

[8] T. Shibata, T. Suzuki, Chem. Phys. Lett. 262 (1996) 115.
[9] C.O.D. Védova, R.E. Rubio, J. Mol. Struct. 321 (1994) 279.
[10] V.N. Khabashesku, A.K. Maltsev, O.M. Nefedov, J. Anal. Appl. Pyrol. 13 (1988) 135.
[11] A.D. Becke, J. Chem. Phys. 98 (1993) 5648.
[12] C.T. Lee, W.E. Yang, R.G. Parr, Phys. Rev. B37 (1988) 785.
[13] M.J. Frisch et al, Gaussian 03, Revision B.03, Gaussian, Inc., Pittsburgh PA, 2003.
[14] R. Fausto, J.J.C. Teixera-Dias, J. Mol. Struct. 144 (1986) 241.
[15] M.V. Pettersen, L. Schriver-Mazzuoli, A. Schriver, P. Chaquin, E. Lasson, Chem. Phys. 204 (1996) 115.
[16] M.E. Jacox, D.E. Milligan, J. Chem. Phys. 43 (1965) 866.
[17] M.E. Jacox, D.E. Milligan, N.G. Moll, W.E. Thompson, J. Chem. Phys. 43 (1965) 3734.
[18] L. Andrews, J. Chem. Phys. 48 (1968) 972.
[19] G. Maier, H.P. Reisenauer, J. Hu, B.A. Hess, Jr., L.J. Schaad, Tetrahedron Lett. 30 (1989) 4105.
[20] M.E. Jacox, D.E. Milligan, J. Chem. Phys. 54 (1971) 3935.
[21] S. Hashimoto, H. Akimoto, J. Phys. Chem. 91 (1987) 1347.
[22] K. Johnsson, A. Engdahl, B. Nelander, J. Phys. Chem. 97 (1993) 9603.
[23] H. Pernice, P. Garcia, H. Willner, J.S. Francisco, F.P. Mills, M.Allen, Y.L. Yung, PNAS 101 (2004) 14007.
[24] N.G. Moll, D.R. Clutter, W.E. Thompson, J. Chem. Phys. 45 (1966) 4469.
[25] T.-L. Tso, E.K.C. Lee, J. Phys. Chem. 88 (1984) 5465.

Figure captions

Fig. 1: IR difference spectrum upon UV irradiation on the matrix CCl_3COCl/Ar = 1/1000 for 60 min.

Fig. 2: Time evolution of the parent (Δ) and the yields of photoproduct CCl_3 (□) and CCl_4 (●) measured in the (a) annealed matrix for 30 min at 20 K before irradiation and (b) non-annealed matrix upon reduced irradiation.

Fig. 3: IR difference spectrum upon UV irradiation on the matrix CCl_3COCl/O_2 = 1/1000 for 60 min.

Fig. 4: Energy diagram of the CCl_3COCl chemistry calculated at the (U)B3LYP/aug-cc-pVTZ level.

Fig. 5: Optimized equilibrium structures of S_0, T_1 and S_1 calculated with the HF, UHF and CIS methods, respectively, using the 6-311+(2d) basis set. Bond lengths and angles are in Å and degrees, respectively.

Table 1

FTIR spectra of photochemical reaction products of CCl_3COCl in matrices

Wavenumber / cm^{-1}		Assignment
Ar	O_2	
	2341	CO_2
	2275	$^{13}CO_2$
2155		$Cl_2C=C=O$
2151		$Cl_2C=C=O$
	2144	O_3 $\nu_1+\nu_3$
2139		$Cl_2CCl\cdots Cl\cdots CO$
2137	2137	CO
	2107	O_3 $3\nu_2$
	2097	^{13}CO
	2037	$CO_3\cdots Cl$
1969		CCO
	1888	*trans*-ClC(O)OO
1878		COCl
	1824	*cis*-ClC(O)OO
1814	1816	$COCl_2$
	1436	ClOO
1293		$Cl_2C=C=O$
1287		$Cl_2C=C=O$
	1100	O_3 ν_1
	1038	O_3 ν_3
1036		$Cl_2CCl\cdots Cl\cdots CO$
	954	*cis*-ClC(O)OO
936		$Cl_2C=C=O$
934		$Cl_2C=C=O$
929		$Cl_2CCl\cdots Cl\cdots CO$
	926	*trans*-ClC(O)OO
899		CCl_3
864		$^{13}CCl_3$
	847	ClO
837	841	$COCl_2$
788	791	CCl_4
767	770	CCl_4

703	O_3 ν_2

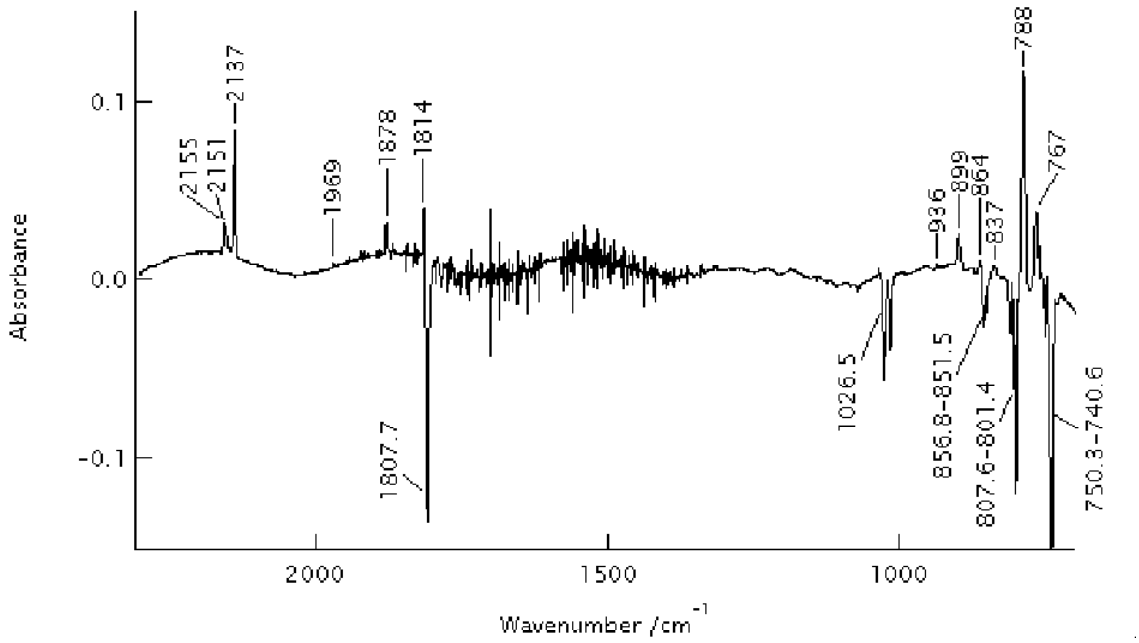
Absorbance
0.1
0.0
-0.1
2155
2151
2137
1969
1878
1814
1807.7
1026.5
936
899
864
856.8-851.5
837
807.6-801.4
788
767
750.3-740.6
2000
1500
1000
Wavenumber /cm-1

Fig. 1

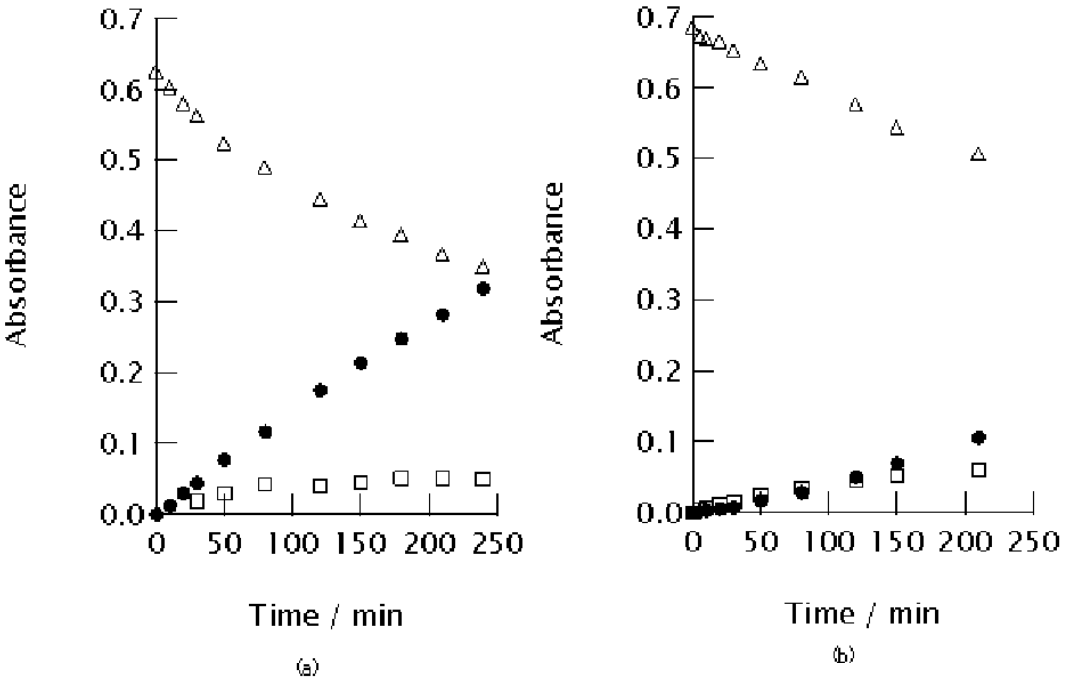
Absorbance
0.7
0.6
0.5
0.4
0.3
0.2
0.1
0.0
0
50
100
150
200
250
Time / min
(a)
Absorbance
0.7
0.6
0.5
0.4
0.3
0.2
0.1
0.0
0
50
100
150
200
250
Time / min
(b)

Fig. 2

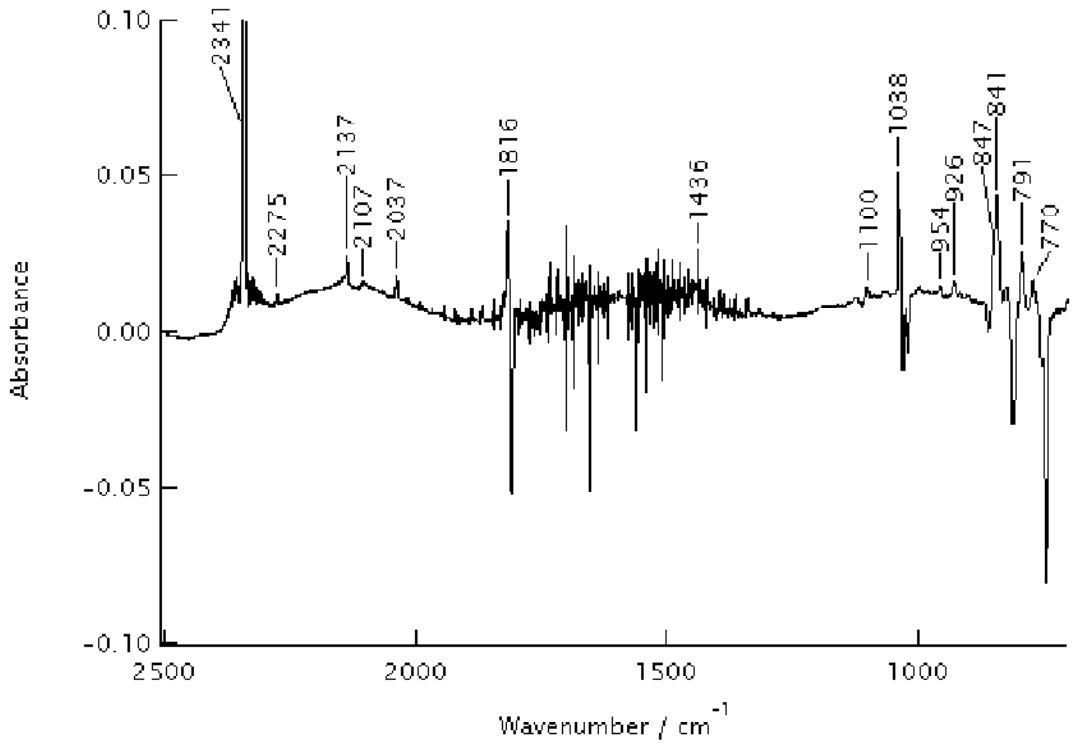
0.10
0.05
0.00
-0.05
-0.10
Absorbance
2500
2000
1500
1000
Wavenumber / cm-1
2341
2275
2137
2107
2037
1816
1436
1100
1038
954
926
847
841
791
770

Fig. 3

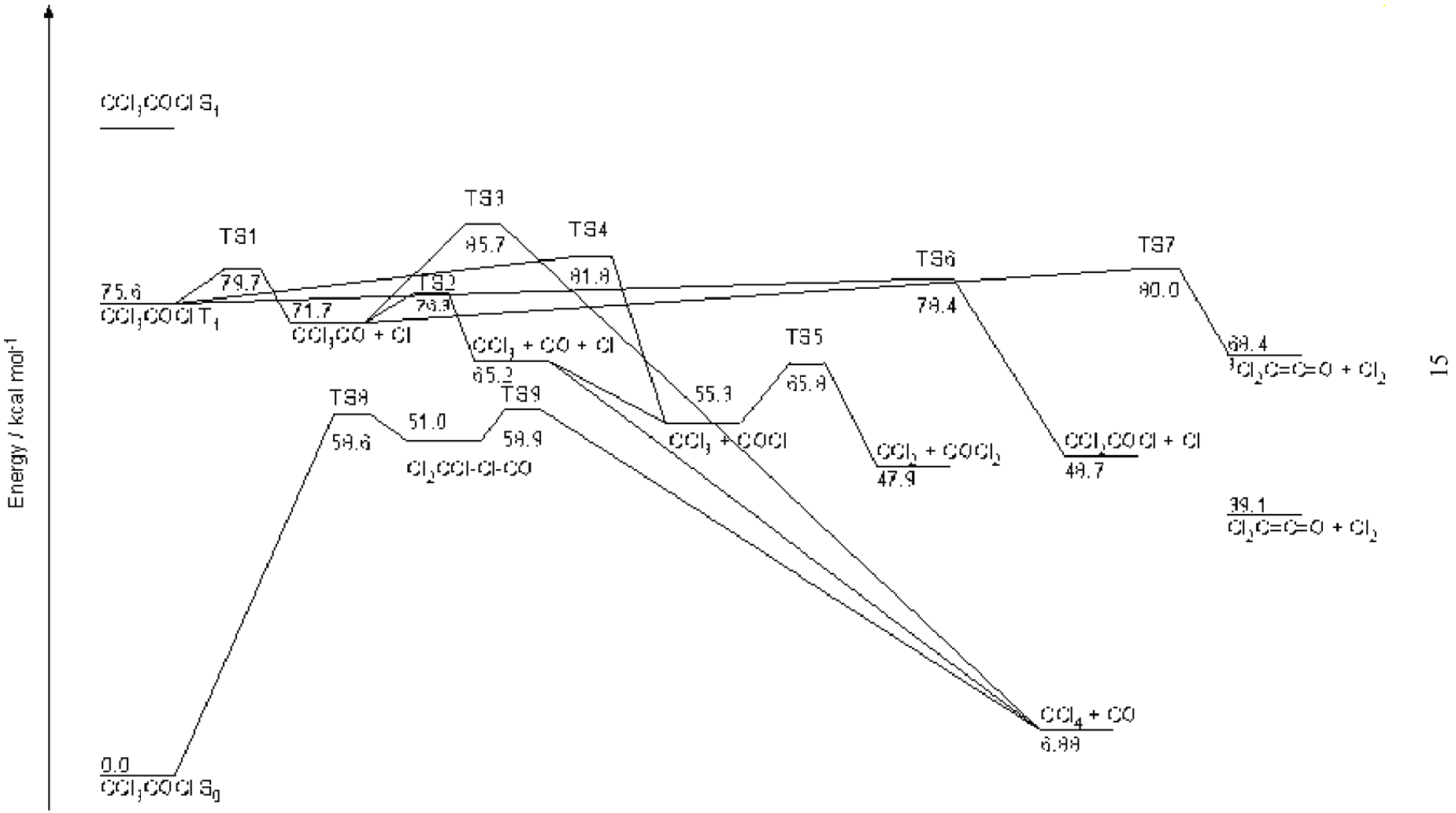
Energy / kcal mol-1
CCl3COCl S1
TS1
TS3
TS4
TS6
TS7
85.7
81.8
80.0
75.6
CCl3COCl T1
79.7
TS2
79.3
71.7
78.4
89.4
Cl2C=C=O + Cl2
CCl3CO + Cl
CCl3 + CO + Cl
65.2
TS5
55.3
65.8
TS8
TS9
51.0
58.6
58.9
CCl3 + COCl
CCl3 + COCl2
CCl3COCl + Cl
47.9
48.7
39.1
Cl2C=C=O + Cl2
CCl4 + CO
6.88
0.0
CCl3COCl S0
Cl2CCl-Cl-CO

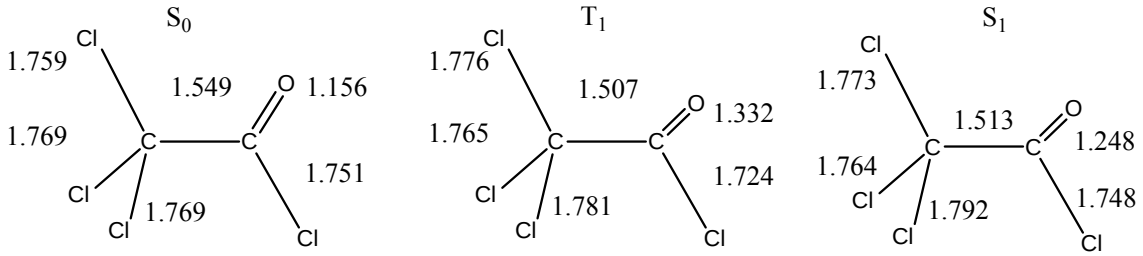

ϕ(CCClO) = 180.0 ϕ(CCClO) = –137.0 ϕ(CCClO) = –141.9

Fig. 5